

# Correlation diagrams of stereoisograms for characterizing stereoisomers of cyclobutane derivatives

Shinsaku Fujita

Received: 28 January 2009 / Accepted: 24 February 2009 / Published online: 14 March 2009  
© Springer Science+Business Media, LLC 2009

**Abstract** Correlation diagrams of stereoisomers are developed as a versatile device for discussing the stereoisomerism of cyclobutane derivatives. A cyclobutane skeleton belongs to an *RS*-stereoisomeric group, which is constructed by starting from the point group  $D_{4h}$  in order to represent a global symmetry. Stereoisomers derived from the cyclobutane skeleton are treated by a main correlation diagram of stereoisograms under the action of the *RS*-stereoisomeric group. In order to discuss the local symmetry of each *RS*-stereogenic center, on the other hand, a promolecule is generated at each *RS*-stereogenic center, where the *RS*-stereoisomeric group for specifying the promolecule is constructed by starting from the point group  $T_d$ . Such promolecules derived from respective stereoisomers are correlated to each other by using stereoisograms, which are further correlated to give a correlation diagram of stereoisograms. *RS*-stereodescriptors are discussed on the basis of such correlation diagrams of stereoisograms.

**Keywords** Cyclobutane · Stereochemistry · *RS*-diastereomeric · *RS*-stereoisomeric · Stereoisogram · Correlation diagram · *RS*-stereodescriptors · Global symmetry · Local symmetry

## 1 Introduction

The concept of “stereogenicity” has not been directly defined in the IUPAC 1996 Recommendations [1] and even in the IUPAC 2004 Provisional Recommendations

---

S. Fujita (✉)  
Shonan Institute of Chemoinformatics and Mathematical Chemistry, Kaneko 479-7,  
Ooimachi, Ashigara-Kami-Gun, Kanagawa-Ken 258-0019, Japan  
e-mail: fujita-sicimc@nifmail.jp

[2, P-91.1.1.1], although it has been regarded as a basis of stereoisomerism and related items such as the Cahn-Ingold-Prelog (CIP) system for specifying *RS*-stereodescriptors [3,4]. Because of such an insufficient definition, the concept of “stereogenicity” has a fundamental drawback: that is to say, it is incapable of deriving the concept of “local stereogenicity”, which would be essential to the CIP system if well-defined. Although the term “stereogenic units” has been defined as a remedy for the insufficient definition, it was also unable to arrive at the concept of “local stereogenicity”. Since the concept of *local chirality* was defined well by means of the term *chirotopic* proposed by Mislow and Siegel [5], the conventional terminology of stereoisomerism tends to rely on the concept of *local chirality*, which has been unconsciously mixed up with “local stereogenicity” to be defined more definitely. As a result, even the revised CIP system [4] as well as the state-of-the-art description of the system [2] has used terms such as “chirality centers” and “stereogenic centers” in a mixed fashion, although they should be replaced by more adequate terms.

Recently, the concept of *RS-stereogenicity* has been developed by Fujita [6,7] as a rigorous concept distinct from *chirality* after stereoisograms were developed as a new device for specifying *RS*-stereoisomerism. The *RS*-stereoisomerism defined as a subconcept of stereoisomerism consists of three relationships, i.e., enantiomeric, *RS*-diastereomeric, and holantimeric relationships, which are respectively correlated to three kinds of properties, i.e., chirality, *RS*-stereogenicity, and sclerality. The distinct definition of *RS*-stereogenicity has permitted us to derive the concept of *local RS-stereogenicity* in a consistent way to the concept of *local chirality* [8]. One of the important conclusions is that the CIP system for specifying *RS*-stereodescriptors is based on *RS*-stereogenicity (especially, local *RS*-stereogenicity), where *RS*-stereodescriptors are given pairwise to two promolecules in an *RS*-diastereomeric relationship, which is distinct from an enantiomeric relationship.

However, the accomplishments described in the preceding paragraph have been mainly concerned with cases having a single *RS*-stereogenic unit. In other words, the relationship between local and global *RS*-stereogenicity as well as between local and global chirality has not been so systematically discussed in complicated cases having multiple *RS*-stereogenic units. Moreover, the relationship between *RS*-stereogenicity (local and global) and chirality (local and global) has been scarcely discussed in such complicated cases, because of the lack of suitable methodology. For example, although the C<sub>1</sub> and C<sub>3</sub> carbons of *cis*-cyclobutane-1,3-diol have been specified by (*1s*, *3s*)-stereodescriptors on the basis of *RS*-stereogenicity, there have been no discussions on how the local/global *RS*-stereogenicity or *RS*-astereogenicity is related to the local/global chirality or achirality.

The discussions in the preceding paragraphs mean that local *RS*-stereogenicity and local chirality should be integrated to the concept of *local symmetry*, where the terms *global (local) symmetry*, *global (local) RS-stereogenicity*, and *global (local) chirality* are used systematically on the basis of *RS*-stereoisomerism reinforced by stereoisograms. The present paper is devoted to an investigation on cases of multiple *RS*-stereogenic centers which are generated from a cyclobutane ring, where *correlation diagrams of stereoisograms* are employed as a key concept.

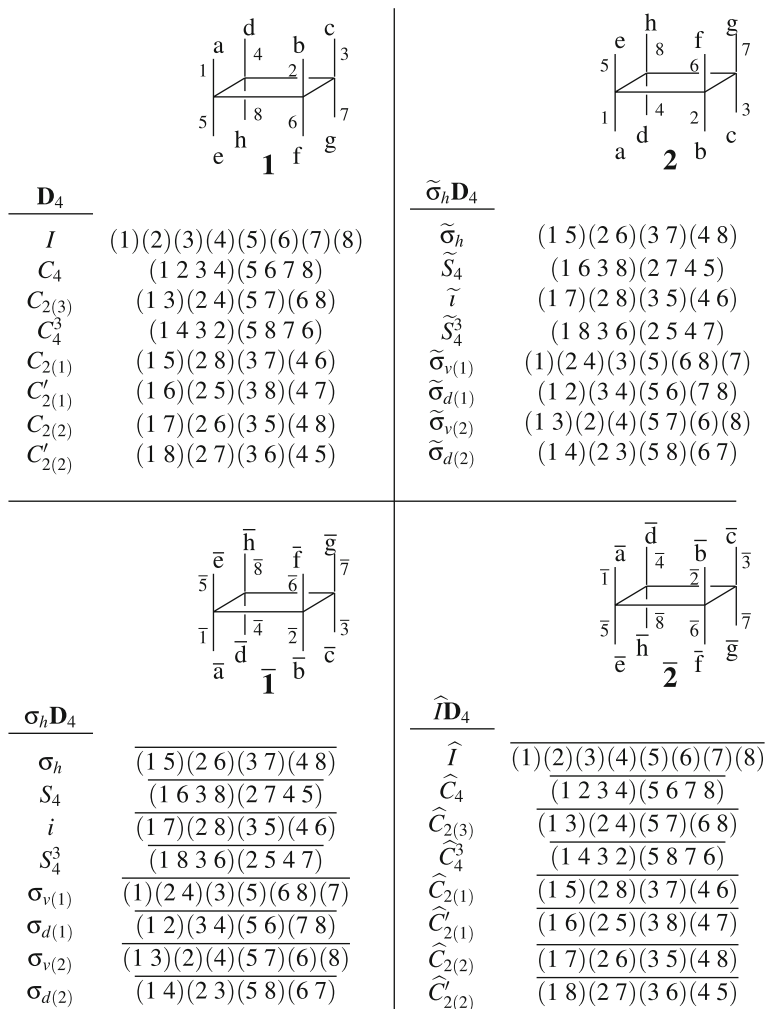


**Fig. 1** *RS*-Stereoisomeric group  $D_{4h}\tilde{\sigma}_h\hat{I}$  derived from a coset representation of  $D_{4h}$  for characterizing cyclobutane derivatives

## 2 Results

### 2.1 *RS*-stereoisomeric groups for cyclobutane derivatives

Let us first examine a cyclobutane ring **1**, where the eight substitution positions are numbered from 1 to 8 as shown in Fig. 1. The mode of numbering is selected arbitrarily from  $8!$  ( $= 40,320$ ) modes of numbering but the selection of any numbering does not lose generality. The cyclobutane ring **1** belongs to a point group  $D_{4h}$  of order 16:

$$\mathbf{D}_{4h} = \{I, C_4, C_{2(3)}, C_4^3, C_{2(1)}, C'_{2(1)}, C_{2(2)}C'_{2(2)}; \sigma_h, S_4, i, S_4^3, \sigma_{v(1)}, \sigma_{d(1)}, \sigma_{v(2)}, \sigma_{d(2)}\}. \quad (1)$$

Following Fujita's USCI (unit-subduced-cycle-index) approach [9], the eight substitution positions of **1** are determined to construct an eight-membered orbit governed by a coset representation  $\mathbf{D}_{4h}/(\mathbf{C}_s)$  of degree 8 ( $= |\mathbf{D}_{4h}|/|\mathbf{C}_s| = 16/2$ ). Its concrete form is collected in the left part of Fig. 1 in the form of products of cycles, where an oberbar indicates the alternation of the configuration of each proligand. For a discussion on coset representations and a mark table of  $\mathbf{D}_{4h}$ , see Ref. [10].

The point group  $\mathbf{D}_{4h}$  is composed of two cosets in terms of its subgroup  $\mathbf{D}_4$ :

$$\mathbf{D}_{4h} = \mathbf{D}_4 + \sigma_h \mathbf{D}_4, \quad (2)$$

where each element is equalized to the corresponding permutation of the coset representation  $\mathbf{D}_{4h}/(\mathbf{C}_s)$ . Suppose that  $\tilde{\sigma}_h$  denotes the same permutation as  $\sigma_h$  but with no alternation of ligand configurations and that  $\hat{I}$  denotes the same permutation as  $I$  but with the alternation of ligand configurations. Thereby, there appear two additional groups derived from  $\mathbf{D}_{4h}$  as follows:

$$\mathbf{D}_{4\tilde{\sigma}} = \mathbf{D}_4 + \tilde{\sigma}_h \mathbf{D}_4, \quad (3)$$

$$\mathbf{D}_{4\hat{I}} = \mathbf{D}_4 + \hat{I} \mathbf{D}_4. \quad (4)$$

By following the formulation by Fujita [7, 11, 12], the resulting cosets,  $\mathbf{D}_4$ ,  $\sigma_h \mathbf{D}_4$ ,  $\tilde{\sigma}_h \mathbf{D}_4$ , and  $\hat{I} \mathbf{D}_4$  are collected to give an *RS*-stereoisomeric group:

$$\mathbf{D}_{4h\tilde{\sigma}\hat{I}} = \mathbf{D}_4 + \sigma_h \mathbf{D}_4 + \tilde{\sigma}_h \mathbf{D}_4 + \hat{I} \mathbf{D}_4, \quad (5)$$

whose concrete elements are shown in Fig. 1.

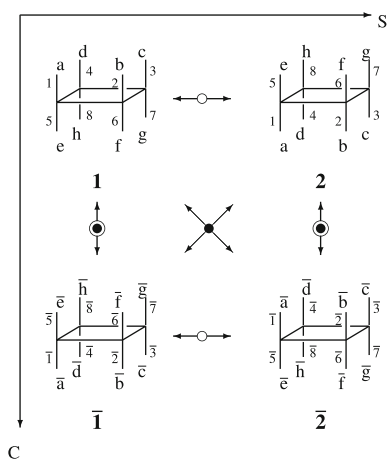
Because  $\mathbf{D}_4$  is a normal subgroup of the resulting *RS*-stereoisomeric group  $\mathbf{D}_{4h\tilde{\sigma}\hat{I}}$ , the coset decomposition represented by Eq. 5 generates the following factor group:

$$\mathbf{D}_{4h\tilde{\sigma}\hat{I}}/\mathbf{D}_4 = \{\mathbf{D}_4, \sigma_h \mathbf{D}_4, \tilde{\sigma}_h \mathbf{D}_4, \hat{I} \mathbf{D}_4\}. \quad (6)$$

By applying a general formulation by Fujita [13] to this special case, the four cosets at issue are shown to correspond to four promolecules **1**,  $\bar{\mathbf{1}}$ , **2**, and  $\bar{\mathbf{2}}$ , as shown in Fig. 1, where the eight positions of each promolecule accommodate a set of eight proligands selected from pairs of enantiomeric proligands in isolation:  $a/\bar{a}$ ,  $b/\bar{b}$ , . . . , and  $h/\bar{h}$ . Note that the promolecule **1** is a representative of eight promolecules (homomers) generated by the action of the eight permutations of  $\mathbf{D}_4$ , the promolecule  $\bar{\mathbf{1}}$  is a representative of eight promolecules (homomers) generated by the action of the eight permutations of  $\sigma_h \mathbf{D}_4$ , and so on.

The promolecules illustrated in Fig. 1 are arranged to give a quadruplet, which constructs a stereoisogram shown in Fig. 2, where an enantiomeric relationship between **1** and  $\bar{\mathbf{1}}$ , an *RS*-diastereomeric relationship between **1** and **2**, and a holantimeric relationship between **1** and  $\bar{\mathbf{2}}$  are denoted by double-headed arrows with respective symbols.

**Fig. 2** Type III stereoisogram of a cyclobutane derivative. The symbols  $a/\bar{a}$ ,  $b/\bar{b}$ , ..., and  $h/\bar{h}$  denote pairs of enantiomeric proligands in isolation



The stereoisogram of Fig. 2 belongs to Type III according to the formulation reported in Ref. [6].

The factor group  $\mathbf{D}_{4h\tilde{\sigma}\hat{I}}/\mathbf{D}_4$  (Eq. 6) corresponds to the following transversal:

$$\mathbf{C}_{h\tilde{\sigma}\hat{I}} = \{I, \sigma_h, \tilde{\sigma}_h, \hat{I}\}, \quad (7)$$

$$\sim \{(1)(2)(3)(4)(5)(6)(7)(8), \overline{(1\ 5)(2\ 6)(3\ 7)(4\ 8)}, \\ (1\ 5)(2\ 6)(3\ 7)(4\ 8), \overline{(1)(2)(3)(4)(5)(6)(7)(8)}\}. \quad (8)$$

where multiplications of respective elements are represented by  $\sigma_h\tilde{\sigma}_h = \hat{I}$ ,  $\tilde{\sigma}_h\hat{I} = \sigma_h$ ,  $\sigma_h\hat{I} = \tilde{\sigma}_h$ , and so on. Obviously, the transversal  $\mathbf{C}_{h\tilde{\sigma}\hat{I}}$  is a group, which is isomorphic to the factor group  $\mathbf{D}_{4h\tilde{\sigma}\hat{I}}/\mathbf{D}_4$ . As a result, the group  $\mathbf{C}_{h\tilde{\sigma}\hat{I}}$  (Eq. 7 or Eq. 8) can be regarded as governing the stereoisogram shown in Fig. 2.

## 2.2 Main stereoisograms for characterizing global symmetries

The global symmetries (global *RS*-stereogenicity and global chirality) of a molecule are characterized by a stereoisogram [6], which is called here *a main stereoisogram*. For example, by placing two chlorine atoms on the positions 1 and 2 and six hydrogen atoms on the remaining positions in each promolecule contained in Fig. 2, we obtain *cis*-1,2-dichlorocyclobutane **3** shown in Fig. 3a. Because the four promolecules Fig. 3a are identical, the main stereoisogram of **3** belongs to Type IV (achiral/*RS*-astereogenic/ascleral) according to the categorization scheme reported in Ref. [6]. In other words, **3** belongs to the maximal subgroup of  $\mathbf{C}_{h\tilde{\sigma}\hat{I}}$  (Eq. 7), i.e.,  $\mathbf{C}_{h\tilde{\sigma}\hat{I}}$  itself.

To characterize *trans*-1,2-dichlorocyclobutane, another mode of numbering is adopted as shown in Fig. 3b, where two chlorine atoms are placed on the positions 1 and 2 and six hydrogen atoms are placed on the remaining positions. The resulting stereoisogram of *trans*-1,2-dichlorocyclobutane (Fig. 3b) belongs to Type I (chiral/*RS*-stereogenic/ascleral). More definitely speaking, **4** (or  $\bar{\mathbf{4}}$ ) belongs to the subgroup  $\{I, \hat{I}\}$  of  $\mathbf{C}_{h\tilde{\sigma}\hat{I}}$  (Eq. 7).

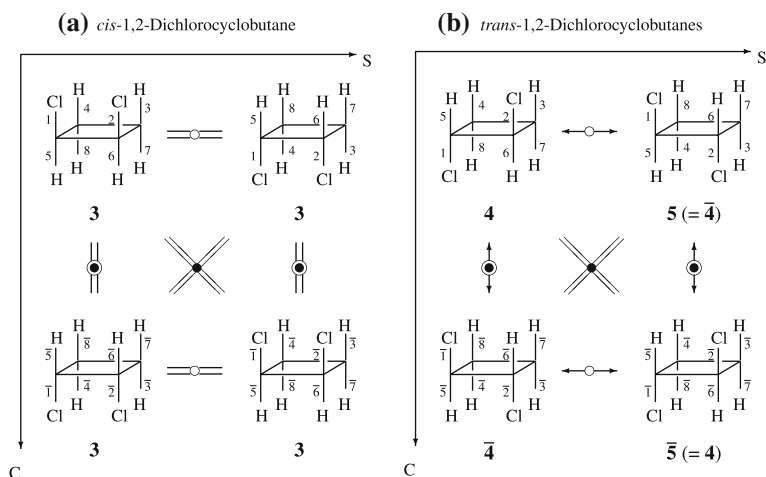


**Fig. 3** A main stereoisogram (Type IV) of *cis*-1,2-dichlorocyclobutane and a main stereoisogram (Type I) of *trans*-1,2-dichlorocyclobutanes

It should be noted the mode of numbering adopted in Fig. 3b generates another coset representation different from the coset representation collected in Fig. 1. In order to treat stereoisomerism between *cis*- and *trans*-1,2-dichlorocyclobutanes, such different coset representations corresponding to Fig. 3a and b should be investigated by examining the symmetric group of degree 8 or its appropriate subgroup. When we extend the *RS*-stereoisomeric group  $\mathbf{D}_{4h\tilde{\sigma}\tilde{\tau}}$  by the following coset decomposition:

$$\mathbf{G} = \mathbf{D}_{4h\tilde{\sigma}\tilde{\tau}} + (1\ 5)\mathbf{D}_{4h\tilde{\sigma}\tilde{\tau}}, \quad (9)$$

we are able to discuss *cis*- and *trans*-1,2-dichlorocyclobutanes on a common basis, where the coset  $(1\ 5)\mathbf{D}_{4h\tilde{\sigma}\tilde{\tau}}$  is stabilized by the  $(1\ 5)\mathbf{D}_{4h\tilde{\sigma}\tilde{\tau}}(1\ 5) (= \mathbf{D}_{4h\tilde{\sigma}\tilde{\tau}})$ . Because this way is tedious, the present paper takes another succinct way using stereoisograms extensively, where the two stereoisograms (Fig. 3a and b) are considered to be independent under the action of  $\mathbf{D}_{4h\tilde{\sigma}\tilde{\tau}}$ .

On a similar line, *cis*- and *trans*-1,3-dichlorocyclobutanes (Fig. 4) are generated by the procedure that two chlorine atoms are placed on the positions 1 and 3 and six hydrogen atoms are placed on the remaining positions, where the modes of numbering are common to those adopted in Fig. 3. The global symmetries (global *RS*-stereogenicity and global chirality) of *cis*- and *trans*-1,3-dichlorocyclobutanes are characterized by the main stereoisograms shown in Fig. 4, both of which belong to Type IV (achiral/*RS*-astereogenic/ascleral).

The main stereoisograms of *cis*- and *trans*-1,2-dichlorocyclobutanes (Fig. 3) are capable of specifying the global symmetry of each compound, i.e., the achirality of the *cis*-isomer by means of the Type IV stereoisogram (Fig. 3a) and the chirality of the *trans*-isomers (an enantiomeric pair) by means of the Type I stereoisogram (Fig. 3b). The specification, however, is not concerned with the stereoisomerism between *cis*- and *trans*-1,2-dichlorocyclobutanes. In other words, the relationship between *cis*- and

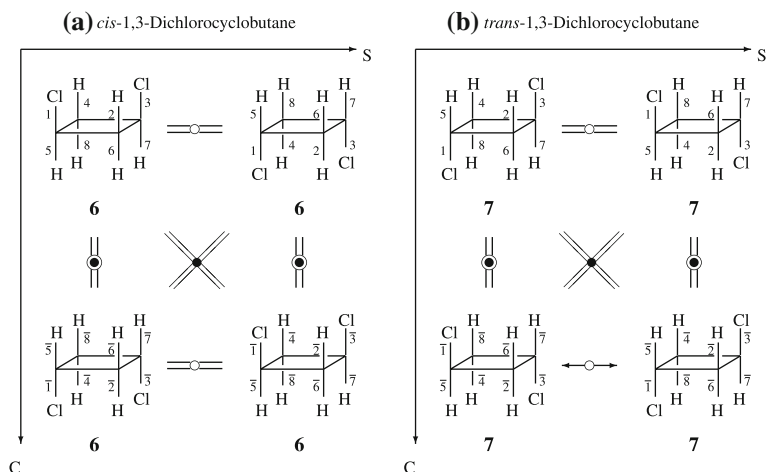


**Fig. 4** A main stereoisogram (Type IV) of *cis*-1,3-dichlorocyclobutane and a main stereoisogram (Type IV) of *trans*-1,3-dichlorocyclobutane

*trans*-1,2-dichlorocyclobutanes is not clarified because there has been no adequate methodology for comparing between Fig. 3a and Fig. 3b. In a parallel way, the stereoisomeric relationship between *cis*- and *trans*-1,3-dichlorocyclobutane is not clarified because of the lack of such an adequate methodology for comparing between Fig. 4a and b. One of the aims of the present paper to show that such an adequate methodology is derived also from the concept of stereoisograms.

## 2.3 Epimeric stereoisograms for characterizing local symmetries

### 2.3.1 Stereoisomerism between *cis*- and *trans*-1,2-dichlorocyclobutanes

*Local symmetries and epimeric stereoisograms* The comparison between the main stereoisograms of *cis*- and *trans*-1,2-dichlorocyclobutanes (Fig. 3) indicates that they are converted into each other by the permutation of position 1 and position 5, which chemically corresponds to an epimerization at the C<sub>1</sub> atom.

Let us look at the C<sub>1</sub> atom of **3**<sub>1</sub> closely as depicted in Fig. 5, where the focused C<sub>1</sub> atom of *cis*-1,2-dichlorocyclobutane (**3**) is denoted by a solid circle. This procedure corresponds to the consideration of the local symmetry at the C<sub>1</sub> atom. The structural formula **3**<sub>1</sub> is converted into a digraph **8** by a ring-opening procedure, which follows a similar procedure adopted in the CIP system [2]. When the right-hand and left-hand residues of **8** are considered to be proligands p and q, we obtain **3**<sub>ℓ1</sub> (a Fischer-like projection) or **3**<sub>p1</sub> (a tetrahedral projection).

On a similar line, the C<sub>1</sub> atom of *trans*-1,2-dichlorocyclobutane (**4**) is focused as depicted in **4**<sub>1</sub>, which is converted into **4**<sub>ℓ1</sub> (a Fischer-like projection) or **4**<sub>p1</sub> (a tetrahedral projection).

By keeping the procedure of Fig. 5 in mind, an epimerization at the C<sub>1</sub> of *cis*- and *trans*-1,2-dichlorocyclobutane is illustrated in two different ways as shown in Fig. 6a.

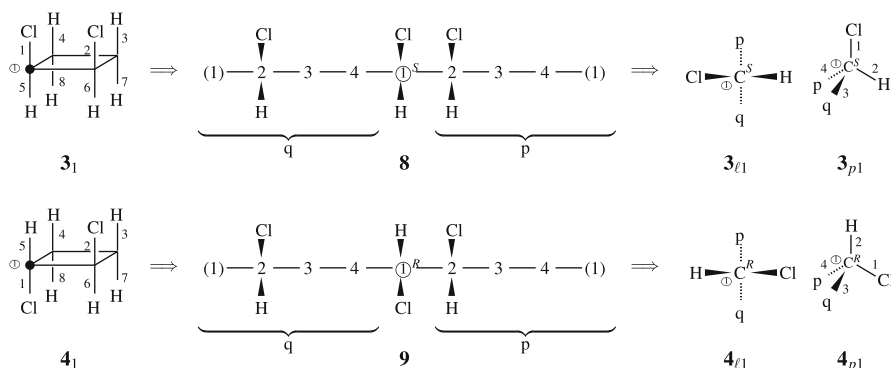


**Fig. 5** Ring opening procedure for converting structural formulas (projective configurations) into tree-equivalent diagrams, where the cyclobutane ring is cleaved to give a tetrahedral promolecule having two ligands  $p$  (or  $\bar{p}$ ) and  $q$  (or  $\bar{q}$ ) which denote resulting open-chains residues. The resulting promolecules specify  $RS$ -stereodescriptors at the  $C_1$  atoms of *cis*- and *trans*-1,2-dichlorocyclobutane

1. The epimerization is considered to correspond to the diastereomeric relationship between  $\mathbf{3}_1$  and  $\mathbf{4}_1$  in the left stereoisogram Fig. 6a, which represents the local symmetries (local chirality and local  $RS$ -stereogenicity) at the  $C_1$  atom. The quadruplet of the promolecules ( $\mathbf{3}_1$ ,  $\mathbf{4}_1$ ,  $\bar{\mathbf{3}}_1$ , and  $\bar{\mathbf{4}}_1$ ) in the left stereoisogram of Fig. 6a is governed by the following group:

$$C_{E1} = \{(1)(2)(3)(4)(5)(6)(7)(8), \overline{(1\ 5)(2\ 6)(3\ 7)(4\ 8)}, \\ (1\ 5)(2)(3)(4)(6)(7)(8), \overline{(1)(5)(2\ 6)(3\ 7)(4\ 8)}\}, \quad (10)$$

which describes the epimerization by putting

$$I \sim (1)(2)(3)(4)(5)(6)(7)(8), \quad \sigma_h \sim \overline{(1\ 5)(2\ 6)(3\ 7)(4\ 8)}, \\ \bar{\sigma}_h \sim (1\ 5)(2)(3)(4)(6)(7)(8), \quad \text{and} \quad \hat{I} \sim \overline{(1)(5)(2\ 6)(3\ 7)(4\ 8)}.$$

It is to be noted that  $\mathbf{3}_1$  and  $\bar{\mathbf{3}}_1$  are different (enantiomeric) so as to represent the local symmetry at the  $C_1$  although they correspond to the same achiral molecule, i.e., *cis*-1,2-dichlorocyclobutane. The local chirality is different to the global achirality of *cis*-1,2-dichlorocyclobutane. On the other hand, another pair of enantiomeric promolecules,  $\mathbf{4}_1$  and  $\bar{\mathbf{4}}_1$ , corresponds to a pair of enantiomeric *trans*-1,2-dichlorocyclobutanes, i.e.,  $\mathbf{4}$  and  $\bar{\mathbf{4}}$ . Thus, the local chirality appears as a result of the global chirality of *trans*-1,2-dichlorocyclobutanes.

2. The epimerization is also considered to correspond to the  $RS$ -diastereomeric relationship between  $\mathbf{3}_{p1}$  and  $\mathbf{4}_{p1}$  in the right stereoisogram Fig. 6a, which alternatively represents the local symmetries (local chirality and local  $RS$ -stereogenicity) at the  $C_1$  atom of tetrahedral promolecules. The quadruplet of the promolecules ( $\mathbf{3}_{p1}$ ,  $\mathbf{4}_{p1}$ ,  $\bar{\mathbf{3}}_{p1}$ , and  $\bar{\mathbf{4}}_{p1}$ ) in the right stereoisogram of Fig. 6a is governed by the following group:



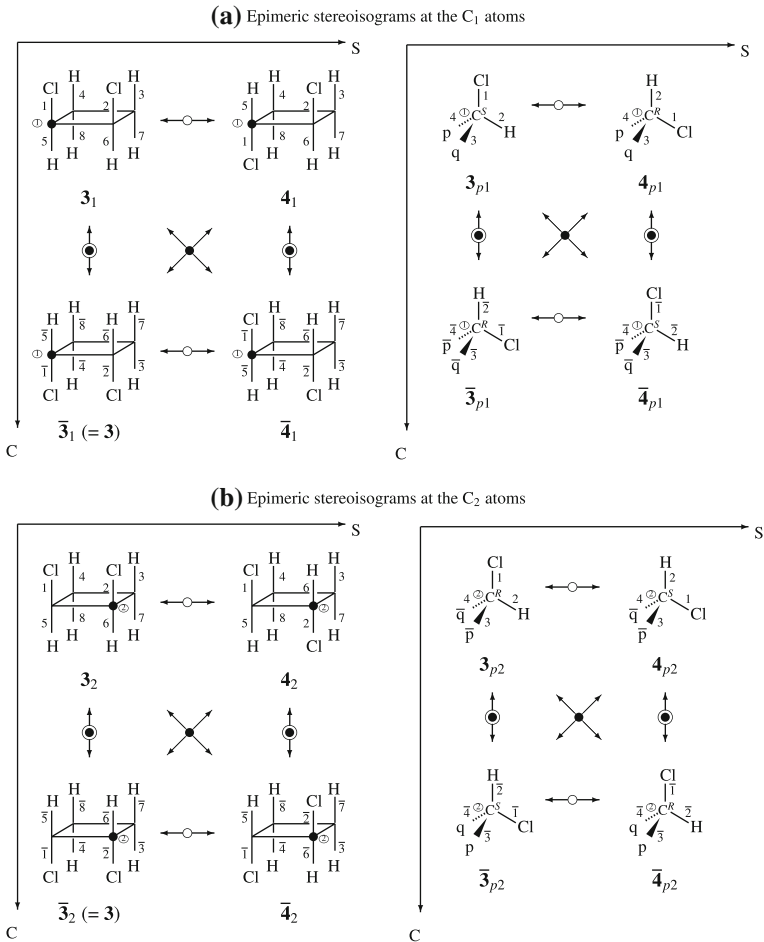


**Fig. 6** Epimeric stereoisograms (Type III) at the C<sub>1</sub> and C<sub>2</sub> atoms of *cis*- and *trans*-1,2-dichlorocyclobutane derivatives. Each left stereoisogram adopts structural formulas (projective configurations), where the focused C<sub>1</sub> (or C<sub>2</sub>) atom is emphasized by a solid circle. Each right stereoisogram represents a tree-equivalent diagram, where the cyclobutane ring is cleaved to give a tetrahedral promolecule having two ligands p (or  $\bar{p}$ ) and q (or  $\bar{q}$ ) which denote resulting open-chains residues

$$\mathbf{G}_{E1} = \{(1)(2)(3)(4), \overline{(1\ 2)(3)(4)}, (1\ 2)(3)(4), \overline{(1)(2)(3)(4)}\}, \quad (11)$$

which describes the epimerization by putting

$$I \sim (1)(2)(3)(4), \quad \sigma_v \sim \overline{(1\ 2)(3)(4)}, \\ \tilde{\sigma}_v \sim (1\ 2)(3)(4), \quad \text{and} \quad \hat{I} \sim \overline{(1)(2)(3)(4)}.$$

The four elements ( $I$ ,  $\sigma_v$ ,  $\tilde{\sigma}_v$ , and  $\hat{I}$ ) are the transversal selected from the coset decomposition of from the  $RS$ -stereoisomeric group  $\mathbf{T}_{d\tilde{\sigma}\hat{I}}$  (derived from  $\mathbf{T}_d$ ) by its subgroup  $\mathbf{T}$  by following a previous formulation [7, 14].

It should be emphasized that the group  $\mathbf{C}_{E1}$  (Eq. 10) for the left stereoisogram Fig. 6a and the group  $\mathbf{G}_{E1}$  (Eq. 11) for the right stereoisogram Fig. 6a are isomorphic to each other, although the original  $RS$ -stereoisomeric groups,  $\mathbf{D}_{4h\tilde{\sigma}\hat{I}}$  and  $\mathbf{T}_{d\tilde{\sigma}\hat{I}}$ , are not isomorphic. Such isomorphism generally holds true because of the isomorphism between factor groups, i.e.,  $\mathbf{D}_{4h\tilde{\sigma}\hat{I}}/\mathbf{D}_4$  and  $\mathbf{T}_{d\tilde{\sigma}\hat{I}}/\mathbf{T}$  in this case [13].

In a parallel way, an epimerization at the  $C_2$  of *cis*- and *trans*-1,2-dichlorocyclobutanes is illustrated in two different ways as shown in Fig. 6b. The quadruplet of the promolecules ( $\mathbf{3}_2$ ,  $\mathbf{4}_2$ ,  $\bar{\mathbf{3}}_2$ , and  $\bar{\mathbf{4}}_2$ ) in the left stereoisogram of Fig. 6b is governed by the following group:

$$\mathbf{C}_{E2} = \{(1)(2)(3)(4)(5)(6)(7)(8), \overline{(1\ 5)(2\ 6)(3\ 7)(4\ 8)}, \\ (2\ 6)(1)(3)(4)(5)(7)(8), \overline{(1\ 5)(2)(6)(3\ 7)(4\ 8)}\}. \quad (12)$$

On the other hand, the quadruplet of the promolecules ( $\mathbf{3}_{p2}$ ,  $\mathbf{4}_{p2}$ ,  $\bar{\mathbf{3}}_{p2}$ , and  $\bar{\mathbf{4}}_{p2}$ ) in the right stereoisogram of Fig. 6b is governed by the group  $\mathbf{G}_{E2}$ , which is essentially the same group as described for the  $C_1$  atom, i.e., Eq. 11.

*RS-stereodescriptors for cis- and trans-1,2-dichlorocyclobutanes* The configuration at the  $C_1$  atom of *cis*-1,2-dichlorocyclobutane is determined by referring to the  $RS$ -diastereomeric relationship between  $\mathbf{3}_{p1}$  and  $\mathbf{4}_{p1}$  in the right stereoisogram of Fig. 6a. The configuration of  $\mathbf{3}_{p1}$  (for *cis*-1,2-dichlorocyclobutane) is determined to be *S* by means of the priority sequence  $\text{Cl} > \text{p} > \text{q} > \text{H}$ . On the other hand, the configuration of  $\mathbf{4}_{p1}$  (for *trans*-1,2-dichlorocyclobutane) is determined to be *R* by means of the common priority sequence  $\text{Cl} > \text{p} > \text{q} > \text{H}$ . This procedure is based on the ring-opening procedure shown in Fig. 5, where  $\mathbf{3}_{p1}$  is regarded as being equivalent to the ring-opening formula **8**. Note that the latter formula **8** corresponds to the digraph used in the CIP system (see Ref. [2]). It should be pointed out that the  $RS$ -stereodescriptors are pairwise given to  $\mathbf{3}_{p1}$  and  $\mathbf{4}_{p1}$ , which are in an  $RS$ -diastereomeric relationship, not in an enantiomeric relationship. On a similar line, the  $RS$ -diastereomeric relationship between  $\mathbf{3}_{p2}$  and  $\mathbf{4}_{p2}$  (the right stereoisogram of Fig. 6b) turns out to give an *R*-configuration to  $\mathbf{3}_{p2}$  and an *S*-configuration to  $\mathbf{4}_{p2}$ . In summary, the abovementioned procedures determine (1*S*, 2*R*) for **3** and (1*R*, 2*S*) for **4**:

- 3**: (1*S*, 2*R*)-1,2-dichlorocyclobutane (not preferred) and  
**4**: (1*R*, 2*S*)-1,2-dichlorocyclobutane,

where the assignment of **3** is not preferred as described below.

Let us next examine the  $RS$ -diastereomeric relationship between  $\bar{\mathbf{3}}_{p1}$  and  $\bar{\mathbf{4}}_{p1}$  in the right stereoisogram of Fig. 6a. The configurations of  $\bar{\mathbf{3}}_{p1}$  (for *cis*-1,2-dichlorocyclobutane) and of  $\bar{\mathbf{4}}_{p1}$  (for *trans*-1,2-dichlorocyclobutane) are determined pairwise to be *R* and *S* by means of the common priority sequence  $\text{Cl} > \bar{\text{p}} > \bar{\text{q}} > \text{H}$ . The  $RS$ -diastereomeric relationship between  $\bar{\mathbf{3}}_{p2}$  and  $\bar{\mathbf{4}}_{p2}$  in the right stereoisogram of Fig. 6b gives *S*- and *R*-configuration. As a result, we obtain (1*R*, 2*S*) for  $\bar{\mathbf{3}}$  and (1*S*, 2*R*) for  $\bar{\mathbf{4}}$ :

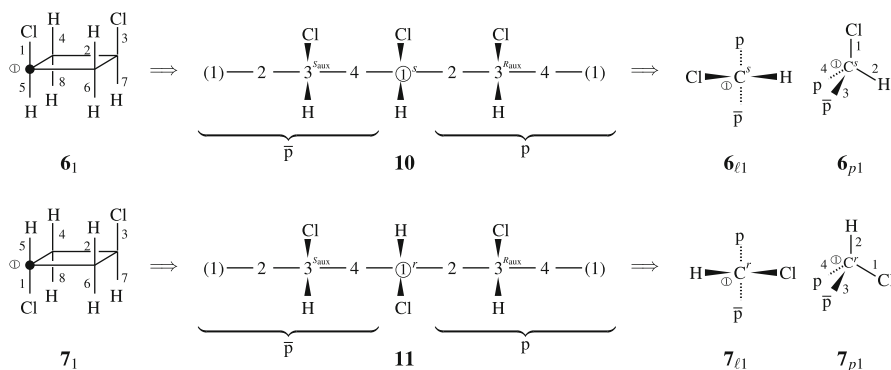


**Fig. 7** Ring opening procedure for converting structural formulas (projective configurations) into tree-equivalent diagrams, where the cyclobutane ring is cleaved to give a tetrahedral promolecule having two ligands  $p$  and  $\bar{p}$  which denote resulting open-chains residues. The resulting promolecules specify  $RS$ -stereodescriptors at the  $C_1$  atoms of *cis*- and *trans*-1,3-dichlorocyclobutane

$\bar{3}$ : (1*R*, 2*S*)-1,2-dichlorocyclobutane and

$4$ : (1*S*, 2*R*)-1,2-dichlorocyclobutane

Because  $3$  is achiral (i.e.,  $3 = \bar{3}$ ), either one of the two possibility for  $3$ , i.e., the (1*S*, 2*R*)-stereodescriptor pair (determined by  $3_{p1}$  and  $3_{p2}$ ) and the (1*R*, 2*S*)-stereodescriptor pair (determined by  $\bar{3}_{p1}$  and  $\bar{3}_{p2}$ ) should be selected in an adequate rule. The latter is usually selected by considering the preference of 1*R* over 1*S*.

### 2.3.2 Stereoisomerism between *cis*- and *trans*-1,3-dichlorocyclobutanes

*Local symmetries and epimeric stereoisograms* Comparison between the main stereoisograms of *cis*- and *trans*-1,3-dichlorocyclobutanes (Fig. 4a and b) shows that they can be converted into each other by the permutation between position 1 and position 5, which corresponds chemically to an epimerization at the  $C_1$  atom.

In a similar way to the ring-opening procedure shown in Fig. 5, the ring opening at the  $C_1$  atom (denoted by a solid circle) of *cis*-1,3-dichlorocyclobutane correlates the promolecule  $6_1$  to another type of expressions  $6_{l1}$  or  $6_{p1}$  via a digraph  $10$ , as shown in the top row of Fig. 7. Note that the right-hand and left-hand residues of  $10$  are considered to be an enantiomeric pair of proligands  $p$  and  $\bar{p}$ , because the residue along the anti-clockwise peripheral path (for  $p$ ) and the other residue along the clockwise peripheral path (for  $\bar{p}$ ) are paired to have mirror-image properties. Similarly, the promolecule  $7_1$  (for the  $C_1$  atom of *trans*-1,3-dichlorocyclobutane) is correlated to another type of expressions  $7_{l1}$  or  $7_{p1}$  via a digraph  $11$ .

By obeying the conversion of Fig. 7, an epimerization at the  $C_1$  atoms of *cis*- and *trans*-1,3-dichlorocyclobutanes is illustrated in two different ways as shown in Fig. 8a. This is parallel to the treatment described for Fig. 6a.

1. The epimerization is considered to correspond to the diastereomeric relationship between  $6_1$  and  $7_1$  in the left stereoisogram Fig. 8a. The quadruplet of the

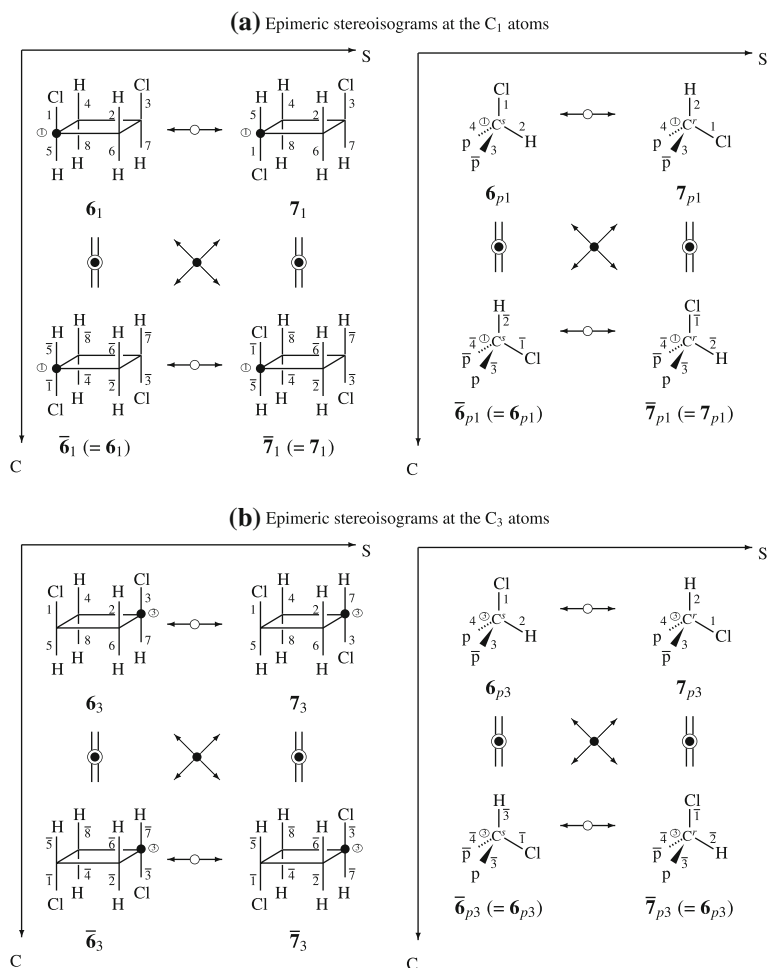


**Fig. 8** Epimeric stereoisograms (Type V) at the C<sub>1</sub> and C<sub>3</sub> atoms of *cis*- and *trans*-1,3-dichlorocyclobutane derivatives. Each left stereoisogram adopts structural formulas (projective configurations), where the focused C<sub>1</sub> (or C<sub>3</sub>) atom is emphasized by a solid circle. Each right stereoisogram represents a tree-equivalent diagram, where the cyclobutane ring is cleaved to give a tetrahedral promolecule having two ligands *p* and  $\bar{p}$  which denote resulting open-chains residues

- promolecules, i.e.,  $\mathbf{6}_1$ ,  $\mathbf{7}_1$ ,  $\bar{\mathbf{6}}_1 (= \mathbf{6}_1)$ , and  $\bar{\mathbf{7}}_1 (= \mathbf{7}_1)$  in the left stereoisogram (Type V) of Fig. 8a, is governed by the subgroup  $\{I, \sigma_h\}$  of the group  $\mathbf{C}_{E1}$  (Eq. 10).
- The epimerization is also considered to correspond to the *RS*-diastereomeric relationship between  $\mathbf{6}_{p1}$  and  $\mathbf{7}_{p1}$  in the right stereoisogram Fig. 8a. The quadruplet of the promolecules, i.e.,  $(\mathbf{6}_{p1}, \mathbf{7}_{p1}, \bar{\mathbf{6}}_{p1} (= \mathbf{6}_{p1}), \text{ and } \bar{\mathbf{7}}_{p1} (= \mathbf{7}_{p1}))$  in the right stereoisogram of Fig. 8a, is governed by the group  $\mathbf{G}_{E1}$  (Eq. 11).

In a parallel way, an epimerization at the C<sub>3</sub> of *cis*- and *trans*-1,3-dichlorocyclobutane is illustrated in two different ways as shown in Fig. 8b. The quadruplet of the promolecules, i.e.,  $\mathbf{6}_3$ ,  $\mathbf{7}_3$ ,  $\bar{\mathbf{6}}_3 (= \mathbf{6}_3)$ , and  $\bar{\mathbf{7}}_3 (= \mathbf{7}_3)$  in the left stereoisogram (Type V) of

Fig. 8b, is governed by the subgroup  $\{(1)(2) \cdots (3), \overline{(1\ 5)(2\ 6)(3\ 7)(4\ 8)}\}$  contained in the following group:

$$\begin{aligned} \mathbf{C}_{E3} = \{ & (1)(2)(3)(4)(5)(6)(7)(8), \overline{(1\ 5)(2\ 6)(3\ 7)(4\ 8)}, \\ & (1)(2)(3\ 7)(4)(5)(6)(8), \overline{(1\ 5)(2\ 6)(3)(7)(4\ 8)}\}, \end{aligned} \quad (13)$$

On the other hand, the quadruplet of the promolecules ( $\mathbf{6}_{p3}$ ,  $\mathbf{7}_{p3}$ ,  $\overline{\mathbf{6}}_{p3}$ , and  $\overline{\mathbf{7}}_{p3}$ ) in the right stereoisogram of Fig. 8b is governed by the subgroup of order 2 contained in the group  $\mathbf{G}_{E3}$ , which is essentially the same group as described for the  $\mathbf{C}_1$  atom, i.e., Eq. 11.

*RS-stereodescriptors for cis- and trans-1,3-dichlorocyclobutanes* The  $\mathbf{C}_1$  atom of *cis*-1,3-dichlorocyclobutane **6** is determined to have *s*-configuration by examining  $\mathbf{6}_{p1}$  in the right stereoisogram of Fig. 8a, where the priority sequence  $\text{Cl} > \text{p} > \overline{\text{p}} > \text{H}$  is employed. According to the CIP sequence rule [2, P-91.3], the preference of the proligand *p* over  $\overline{p}$  is decided by using auxiliary stereodescriptors ( $R_{\text{aux}}$  or  $S_{\text{aux}}$ ), as shown in the digraph **10** (Fig. 7). Because the priority sequence  $\text{Cl} (1) > \text{p} (4) > \overline{\text{p}} (3) > \text{H} (2)$  is changed into  $\text{Cl} (\overline{1}) > \text{p} (3) > \overline{\text{p}} (4) > \text{H} (2)$  (as found in  $\overline{\mathbf{6}}_{p1}$ ), the stereodescriptor is designated in a lowercase letter. The common priority sequence  $\text{Cl} (1) > \text{p} (4) > \overline{\text{p}} (3) > \text{H} (2)$  is applied to  $\mathbf{7}_{p1}$  in the right stereoisogram of Fig. 8a, so that the  $\mathbf{C}_1$  atom of *trans*-1,3-dichlorocyclobutane **7** is determined to have *r*-configuration. It should be emphasized again that a pair of *R*- and *S*-stereodescriptors is given to a pair of  $\mathbf{6}_{p1}$  and  $\mathbf{7}_{p1}$ , which are in an *RS*-diastereomeric relationship as shown in the right stereoisogram of Fig. 8a.

On a similar line, the *RS*-diastereomeric relationship between  $\mathbf{6}_{p3}$  and  $\mathbf{7}_{p3}$  (the right stereoisogram of Fig. 8b) assigns an *s*-configuration to  $\mathbf{6}_{p3}$  and an *r*-configuration to  $\mathbf{7}_{p3}$ , where the priority sequence  $\text{Cl} (1) > \text{p} (4) > \overline{\text{p}} (3) > \text{H} (2)$  is employed.

In summary, the abovementioned procedures assign a descriptor pair (*1s*, *3s*) to *cis*-1,3-dichlorocyclobutane **6** and another descriptor pair (*1r*, *3r*) to *trans*-1,3-dichlorocyclobutane **7**, i.e.,

- 6**: (*1s*, *3s*)-1,3-dichlorocyclobutane and
- 7**: (*1r*, *3r*)-1,3-dichlorocyclobutane

## 2.4 Correlation diagrams of stereoisograms for three *RS*-stereogenic centers

### 2.4.1 Stereoisomerism of 1-bromo-2,3-dichlorocyclobutanes as a non-degenerate case

Cyclobutanes with three *RS*-stereogenic centers require a more sophisticated treatment. To investigate such complicated cases, we here define correlation diagrams of stereoisograms. As a typical example, let us examine stereoisomers of 1-bromo-2,3-dichlorocyclobutane, as shown in Fig. 9.

The global symmetries of the stereoisomers,  $\mathbf{12}/\overline{\mathbf{12}}$ ,  $\mathbf{13}/\overline{\mathbf{13}}$ ,  $\mathbf{15}/\overline{\mathbf{15}}$ , and  $\mathbf{14}/\overline{\mathbf{14}}$ , are represented by a main correlation diagram shown in Fig. 9a, which contains each half

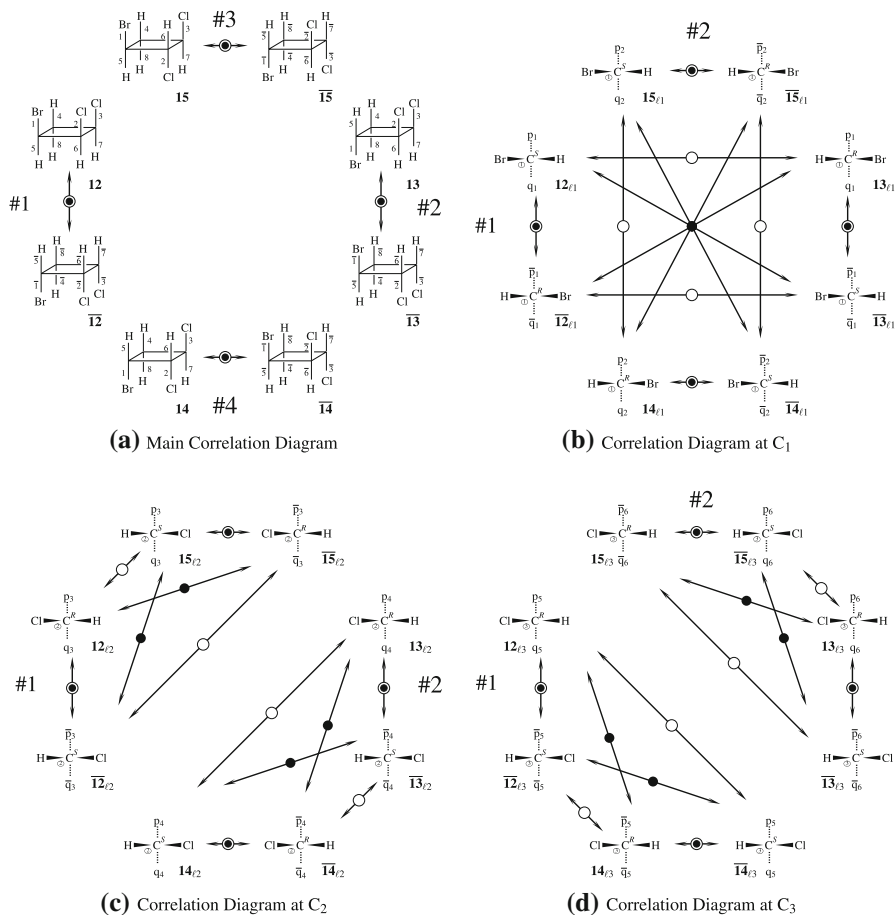


**Fig. 9** Correlation diagrams of stereoisograms for 1-bromo-2,3-dichlorocyclobutane stereoisomers. **a** For the global symmetry: all of the stereoisograms (#1–#4) belong to Type I, where each half part is depicted; **b** for  $C_1$ : stereoisograms of #1 and #2 both belong to Type III, where  $Br > p_i (\bar{p}_i) > q_i (\bar{q}_i) > H$  ( $i = 1, 2$ ); **c** for  $C_2$ : stereoisograms #1 and #2 belong to Type III, where  $Cl > q_i (\bar{q}_i) > p_i (\bar{p}_i) > H$  ( $i = 3, 4$ ); and **d** for  $C_4$ : stereoisograms #1 and #2 belong to Type III, where  $Cl > q_i (\bar{q}_i) > p_i (\bar{p}_i) > H$  ( $i = 5, 6$ )

of their stereoisograms of Type I (#1–#4). The four stereoisograms #1–#4 are independent under the action of respective  $RS$ -stereoisomeric groups, which are isomorphic to  $D_{4h\tilde{\sigma}\tilde{I}}$  (Eq. 5).

When we extend the  $RS$ -stereoisomeric group  $D_{4h\tilde{\sigma}\tilde{I}}$  by considering the following coset decomposition:

$$G' = D_{4h\tilde{\sigma}\tilde{I}} + (1\ 5)D_{4h\tilde{\sigma}\tilde{I}} + (2\ 6)D_{4h\tilde{\sigma}\tilde{I}} + (1\ 5)(2\ 6)D_{4h\tilde{\sigma}\tilde{I}}, \tag{14}$$

we are able to discuss all of the stereoisomers of 1-bromo-1,2-dichlorocyclobutane on a common basis, where the coset  $(1\ 5)D_{4h\tilde{\sigma}\tilde{I}}$  etc. are stabilized by the  $(1\ 5)D_{4h\tilde{\sigma}\tilde{I}}(1\ 5)$  etc., which are identical with  $D_{4h\tilde{\sigma}\tilde{I}}$ . Because this way is tedious, the present paper

takes another succinct way using stereoisograms extensively, where the four stereoisograms #1–#4 are considered to be independent under the action of  $\mathbf{D}_{4h\bar{\sigma}\hat{T}}$ .

By applying a similar procedure of Fig. 5 to this case, the local symmetries at the  $C_1$  atoms of respective stereoisomers are depicted in an epimeric correlation diagram shown in Fig. 9b, which contains two stereoisograms of Type III (#1 and #2). Stereoisogram #1 consists of a quadruplet of  $\mathbf{12}_{\ell 1}/\overline{\mathbf{12}}_{\ell 1}$  and  $\mathbf{13}_{\ell 1}/\overline{\mathbf{13}}_{\ell 1}$ . The *S*-configuration of  $\mathbf{12}_{\ell 1}$  and the *R*-configuration of  $\mathbf{13}_{\ell 1}$  are determined pairwise because they are in an *RS*-diastereomeric relationship, where a common priority sequence  $\text{Br} > p_1 > q_1 > \text{H}$  is used. Their enantiomers, i.e.,  $\overline{\mathbf{12}}_{\ell 1}$  and  $\overline{\mathbf{13}}_{\ell 1}$ , are also in an *RS*-diastereomeric relationship so that they are determined pairwise to have *R*- and *S*-configurations, where another common priority sequence  $\text{Br} > \bar{p}_1 > \bar{q}_1 > \text{H}$  is used.

On the other hand, stereoisogram #2 of Fig. 9b consists of a quadruplet of  $\mathbf{14}_{\ell 1}/\overline{\mathbf{14}}_{\ell 1}$  and  $\mathbf{15}_{\ell 1}/\overline{\mathbf{15}}_{\ell 1}$ . The configurations of  $\mathbf{14}_{\ell 1}$  and of  $\mathbf{15}_{\ell 1}$  in an *RS*-diastereomeric relationship are determined pairwise to be *S* and *R*, where a common priority sequence  $\text{Br} > p_2 > q_2 > \text{H}$  is used. The configurations of  $\overline{\mathbf{14}}_{\ell 1}$  and  $\overline{\mathbf{15}}_{\ell 1}$ , which are in an *RS*-diastereomeric relationship, are determined pairwise to have *R*- and *S*-configuration.

The local symmetries at the  $C_2$  atoms of stereoisomers at issue are depicted in another epimeric correlation diagram shown in Fig. 9c, which contains two stereoisograms of Type III (#1 and #2). Stereoisogram #1 consists of a quadruplet of  $\mathbf{12}_{\ell 2}/\overline{\mathbf{12}}_{\ell 2}$  and  $\mathbf{15}_{\ell 2}/\overline{\mathbf{15}}_{\ell 2}$ . The configurations of  $\mathbf{12}_{\ell 2}$  and of  $\mathbf{15}_{\ell 2}$  in an *RS*-diastereomeric relationship are determined pairwise to be *R* and *S*, where a common priority sequence  $\text{Cl} > q_3 > p_3 > \text{H}$  is used. Their enantiomers, i.e.,  $\overline{\mathbf{12}}_{\ell 2}$  and  $\overline{\mathbf{15}}_{\ell 2}$ , are in an *RS*-diastereomeric relationship so that they are determined pairwise to have *S*- and *R*-configurations, where another common priority sequence  $\text{Cl} > \bar{q}_3 > \bar{p}_3 > \text{H}$  is used.

Stereoisogram #2 of Fig. 9c consists of a quadruplet of  $\mathbf{13}_{\ell 2}/\overline{\mathbf{13}}_{\ell 2}$  and  $\mathbf{14}_{\ell 2}/\overline{\mathbf{14}}_{\ell 2}$ . The configurations of  $\mathbf{13}_{\ell 2}$  and of  $\mathbf{14}_{\ell 2}$  in an *RS*-diastereomeric relationship are determined pairwise to be *R* and *S*, where a common priority sequence  $\text{Br} > q_4 > p_4 > \text{H}$  is used. The configurations of  $\overline{\mathbf{13}}_{\ell 2}$  and  $\overline{\mathbf{14}}_{\ell 2}$ , which are in an *RS*-diastereomeric relationship, are determined pairwise to have *S*- and *R*-configurations.

The local symmetries at the  $C_3$  atoms of respective stereoisomers are depicted in a further epimeric correlation diagram shown in Fig. 9d, which involves two stereoisograms of Type III (#1 and #2). Stereoisogram #1 consists of a quadruplet of  $\mathbf{12}_{\ell 3}/\overline{\mathbf{12}}_{\ell 3}$  and  $\mathbf{14}_{\ell 3}/\overline{\mathbf{14}}_{\ell 3}$ . The configurations of  $\mathbf{12}_{\ell 3}$  and of  $\overline{\mathbf{14}}_{\ell 2}$  in an *RS*-diastereomeric relationship are determined pairwise to be *R* and *S*, where a common priority sequence  $\text{Cl} > q_5 > p_5 > \text{H}$  is used. Because their respective enantiomers, i.e.,  $\overline{\mathbf{12}}_{\ell 2}$  and  $\mathbf{14}_{\ell 3}$  are in an *RS*-diastereomeric relationship, they are determined pairwise to have *S*- and *R*-configurations at the  $C_2$  atoms, where another common priority sequence  $\text{Cl} > \bar{q}_5 > \bar{p}_5 > \text{H}$  is used.

Stereoisogram #2 of Fig. 9d consists of a quadruplet of  $\mathbf{13}_{\ell 3}/\overline{\mathbf{13}}_{\ell 3}$  and  $\mathbf{15}_{\ell 3}/\overline{\mathbf{15}}_{\ell 3}$ . The configurations of  $\mathbf{13}_{\ell 3}$  and of  $\overline{\mathbf{15}}_{\ell 3}$  in an *RS*-diastereomeric relationship are determined pairwise to be *R* and *S*, where a common priority sequence  $\text{Cl} > q_6 > p_6 > \text{H}$  is used. The configurations of  $\overline{\mathbf{13}}_{\ell 3}$  and  $\mathbf{15}_{\ell 3}$ , which are in an *RS*-diastereomeric relationship, are determined pairwise to have *S*- and *R*-configurations.

The assignments of *RS*-stereodescriptors shown in Fig. 9 are summarized as follows:

- 12**: (1*S*, 2*R*, 3*R*)-1-bromo-2,3-dichlorocyclobutane  
**12**: (1*R*, 2*S*, 3*S*)-1-bromo-2,3-dichlorocyclobutane  
**13**: (1*R*, 2*R*, 3*R*)-1-bromo-2,3-dichlorocyclobutane  
**13**: (1*S*, 2*S*, 3*S*)-1-bromo-2,3-dichlorocyclobutane  
**14**: (1*R*, 2*S*, 3*R*)-1-bromo-2,3-dichlorocyclobutane  
**14**: (1*S*, 2*R*, 3*S*)-1-bromo-2,3-dichlorocyclobutane  
**15**: (1*S*, 2*S*, 3*R*)-1-bromo-2,3-dichlorocyclobutane and  
**15**: (1*R*, 2*R*, 3*S*)-1-bromo-2,3-dichlorocyclobutane.

Although the two enantiomers of each pair (e.g., **12/12**) are seemingly pairwise determined to have *RS*-stereodescriptor sets (e.g., (1*S*, 2*R*, 3*R*) vs. (1*R*, 2*S*, 3*S*) for **12/12**), the procedure shown in Fig. 9 indicates that a pair of *R*- and *S*-stereodescriptors is given to a pair of *RS*-diastereomers generated at each *RS*-stereogenic center.

#### 2.4.2 Stereoisomerism of 1,2,3-trichlorocyclobutanes as a degenerate case

The global symmetries of the stereoisomers of 1,2,3-trichlorocyclobutane, **16/16** (= **16**), **17/17**, **19/19** (= **16**), and **18/18** (= **19/19**), are represented by correlation diagrams shown in Fig. 10. The main correlation diagram (Fig. 10a) contains respective halves of their stereoisograms (#1–#4). Stereoisograms #1 and #3 belong to Type IV while #2 and #4 belong to Type I. Note that Stereoisogram #2 and #4 are degenerate under the action of  $G'$  (Eq. 14), where the following subgroup:

$$G'' = D_{4h\tilde{\sigma}\hat{I}} + (2\ 6)D_{4h\tilde{\sigma}\hat{I}} \quad (15)$$

serves as the stabilizer of the two stereoisograms (#2 and #4). In the present approach, however, the four stereoisograms #1–#4 are considered to be independent under the action of  $D_{4h\tilde{\sigma}\hat{I}}$ .

The present degenerate case of 1,2,3-trichlorocyclobutane stereoisomers is examined by starting from the non-degenerate case shown in Fig. 9, where the conversion of cyclobutane derivatives into tetrahedral formulas follows the procedure described in Fig. 5. Thus, the local symmetries at the  $C_1$  atoms of respective stereoisomers are depicted in an epimeric correlation diagram shown in Fig. 10b, which contains two stereoisograms of Type III (#1 and #2). Stereoisogram #1 consists of a quadruplet of **16**<sub>ℓ1</sub>/**16**<sub>ℓ1</sub> and **17**<sub>ℓ1</sub>/**17**<sub>ℓ1</sub>. Although **16**<sub>ℓ1</sub> and **16**<sub>ℓ1</sub> represent the same achiral molecule **16**, they are different from each other in the examination of the local symmetry at the  $C_1$  atom.

The two promolecules in an *RS*-diastereomeric relationship, **16**<sub>ℓ1</sub> and **17**<sub>ℓ1</sub>, are determined pairwise to have *S*- and *R*-configurations, where a common priority sequence Cl > r<sub>1</sub> > s<sub>1</sub> > H is used. Their enantiomers in an *RS*-diastereomeric relationship, i.e., **16**<sub>ℓ1</sub> and **17**<sub>ℓ1</sub>, are in turn determined pairwise to have *R*- and *S*-configurations, where another common priority sequence Cl >  $\bar{r}_1$  >  $\bar{s}_1$  > H is used.

On the other hand, stereoisogram #2 of Fig. 10b consists of a quadruplet of **18**<sub>ℓ1</sub>/**18**<sub>ℓ1</sub> and **19**<sub>ℓ1</sub>/**19**<sub>ℓ1</sub>. The configurations of two promolecules **18**<sub>ℓ1</sub> and of **19**<sub>ℓ1</sub> in an *RS*-diastereomeric relationship are determined pairwise to be *R* and *S*, where a common priority sequence Cl > r<sub>2</sub> > s<sub>2</sub> > H is used. The configurations of **18**<sub>ℓ1</sub> and **19**<sub>ℓ1</sub>,



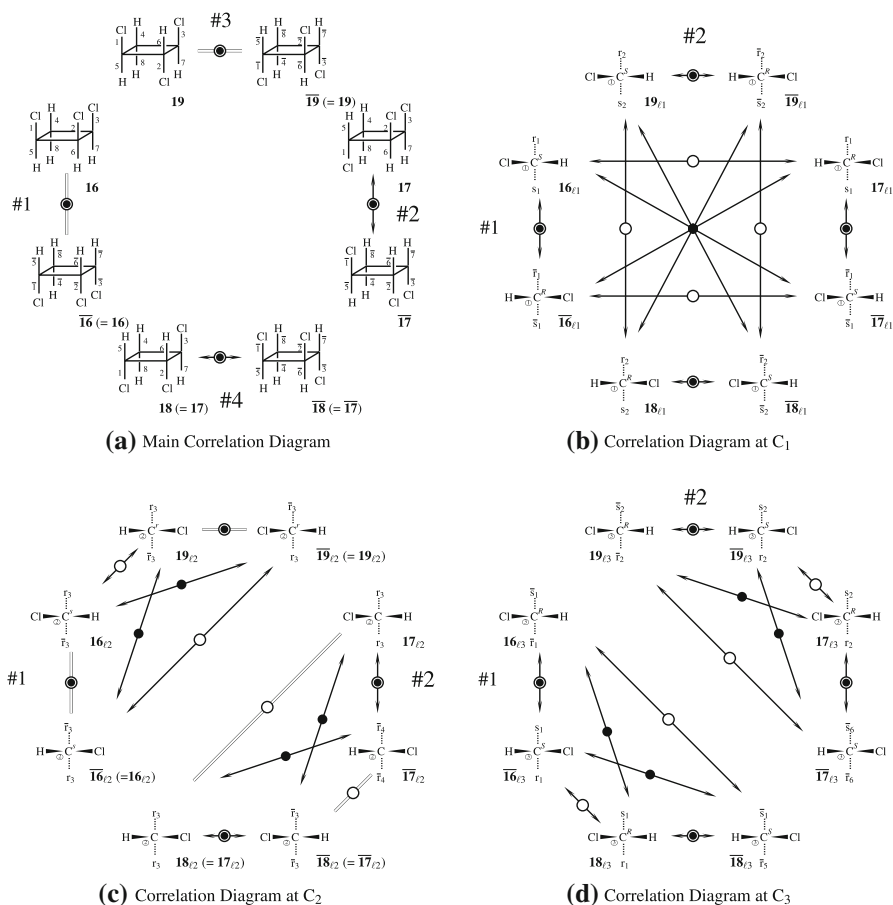


**Fig. 10** Correlation diagrams of stereoisograms for 1,2,3-trichlorocyclobutane stereoisomers. **a** For the global symmetry: stereoisograms #1 and #3 belong to Type IV, while Stereoisograms #2 and #4 belong to Type I, where each half part is depicted; **b** for C<sub>1</sub>: stereoisograms of #1 and #2 both belong to Type III, where Br > r<sub>i</sub> (r̄<sub>i</sub>) > s<sub>i</sub> (s̄<sub>i</sub>) > H (i = 1, 2); **c** for C<sub>2</sub>: stereoisogram #1 belongs to Type V where Cl > r<sub>3</sub> > r̄<sub>3</sub> > H, and stereoisogram #2 belongs to Type II; and **d** for C<sub>3</sub>: stereoisograms #1 and #2 belong to Type III, where Cl > r<sub>i</sub> (r̄<sub>i</sub>) > s<sub>i</sub> (s̄<sub>i</sub>) > H (i = 1, 2)

which are in an *RS*-diastereomeric relationship, are determined pairwise to have *S*- and *R*-configurations.

The local symmetries at the C<sub>2</sub> atoms of stereoisomers at issue are illustrated in another epimeric correlation diagram shown in Fig. 9c, which contains two stereoisograms of Type V and II (#1 and #2). Stereoisogram #1 of Type V consists of a degenerate quadruplet of 16<sub>ℓ2</sub> (= 16̄<sub>ℓ2</sub>) and 19<sub>ℓ2</sub> (= 19̄<sub>ℓ2</sub>), both of which are achiral. Because 16<sub>ℓ2</sub> and of 19<sub>ℓ2</sub> are in an *RS*-diastereomeric relationship, their configurations are determined pairwise to be *s* and *r* by using a common priority sequence Cl > r<sub>3</sub> > r̄<sub>3</sub> > H. Because the priority sequence is chirality unfaithful, the stereodescriptors are designated in lowercase letters *s* and *r*.

Stereoisogram #2 of Type II in Fig. 10c consists of a degenerate quadruplet of  $17_{\ell 2}/\overline{17}_{\ell 2}$  ( $= 18_{\ell 2}/\overline{18}_{\ell 2}$ ). Because of Type II,  $17_{\ell 2}$  (or  $\overline{17}_{\ell 2}$ ) is *RS*-astereogenic so as not to be named by the CIP system.

A further epimeric correlation diagram shown in Fig. 10d illustrates the local symmetry at the  $C_3$  atom of each stereoisomer, where there appear two stereoisograms of Type III (#1 and #2). Stereoisogram #1 consists of a quadruplet of  $16_{\ell 3}/\overline{16}_{\ell 3}$  and  $18_{\ell 3}/\overline{18}_{\ell 3}$ . Because  $16_{\ell 3}$  and  $\overline{18}_{\ell 2}$  are in an *RS*-diastereomeric relationship, their configurations are determined pairwise to be *R* and *S*, where a common priority sequence  $Cl > \bar{r}_1 > \bar{s}_1 > H$  is used. The respective enantiomers, i.e.,  $\overline{16}_{\ell 2}$  and  $18_{\ell 3}$ , are in an *RS*-diastereomeric relationship so that they are determined pairwise to have *S*- and *R*-configurations, where another common priority sequence  $Cl > r_1 > s_1 > H$  is used.

Stereoisogram #2 of Fig. 10d consists of a quadruplet of  $17_{\ell 3}/\overline{17}_{\ell 3}$  and  $19_{\ell 3}/\overline{19}_{\ell 3}$ . The configurations of *RS*-diastereomeric promolecules  $17_{\ell 3}$  and  $19_{\ell 3}$  are determined pairwise to be *R* and *S*, where a common priority sequence  $Cl > r_2 > s_2 > H$  is used. The configurations of  $\overline{17}_{\ell 3}$  and  $19_{\ell 3}$ , which are in an *RS*-diastereomeric relationship, are determined pairwise to have *S*- and *R*-configurations, where a common priority sequence  $Cl > \bar{r}_2 > \bar{s}_2 > H$  is used.

The assignments of *RS*-stereodescriptors shown in Fig. 10 are summarized as follows:

- 16**: (1*S*, 2*s*, 3*R*)-1,2,3-trichlorocyclobutane (achiral, not preferred)
- $\overline{16}$** : (1*R*, 2*s*, 3*S*)-1,2,3-trichlorocyclobutane (achiral)
- 17**: (1*R*, 3*R*)-1,2,3-trichlorocyclobutane
- $\overline{17}$** : (1*S*, 3*S*)-1,2,3-trichlorocyclobutane
- 18**: (1*R*, 3*R*)-1,2,3-trichlorocyclobutane (duplicated)
- $\overline{18}$** : (1*S*, 3*S*)-1,2,3-trichlorocyclobutane (duplicated)
- 19**: (1*S*, 2*r*, 3*R*)-1,2,3-trichlorocyclobutane (achiral, not preferred) and
- $\overline{19}$** : (1*R*, 2*r*, 3*S*)-1,2,3-trichlorocyclobutane (achiral).

The names designated to be “not preferred” or “duplicated” are abandoned because of degeneration. As for the achiral compound **16**, there appear two possibilities, i.e., the descriptor set (1*S*, 2*s*, 3*R*) for **16** and another descriptor set (1*R*, 2*s*, 3*S*) for the tentative enantiomer  **$\overline{16}$**  ( $= 16$ ). The latter is usually selected because of the preference of 1*R* over 1*S*. On the same line, there appear two possibilities for the achiral compound **19**, i.e., the descriptor set (1*S*, 2*r*, 3*R*) for **19** and another descriptor set (1*R*, 2*r*, 3*S*) for the tentative enantiomer  **$\overline{19}$**  ( $= 19$ ). The latter is usually selected because of the preference of 1*R* over 1*S*. These phenomena stem from the fact that **16** and **19** exhibit pseudoasymmetric property, which is demonstrated by stereoisogram #1 of Type V in the epimeric correlation diagram (Fig. 10c).

As found in the main correlation diagram (Fig. 10a), **17** and **18** are identical with each other; and at the same time,  **$\overline{17}$**  and  **$\overline{18}$**  are identical with each other. This fact is also demonstrated by stereoisogram #2 of Type II which appears in the epimeric correlation diagram shown in Fig. 10c. Hence, the names stemmed from **18** and  **$\overline{18}$**  are abandoned because this selection provides the same result as another set of names is selected.

It is to be emphasized again that each pair of *RS*-stereodescriptors due to Fig. 10 is pairwise given to a pair of *RS*-diastereomers. This fact has been overlooked until now

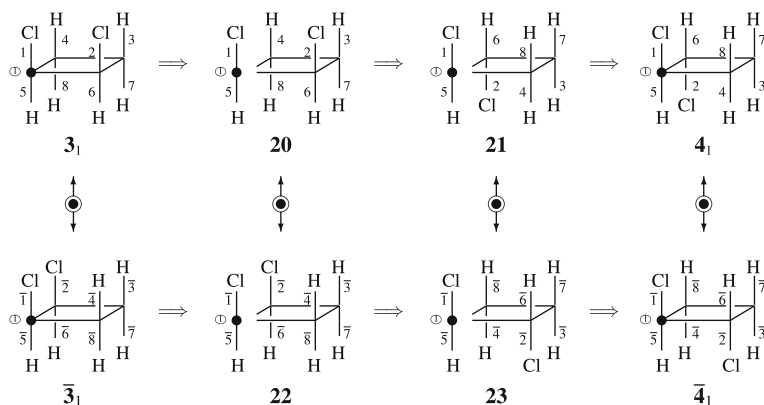


**Fig. 11** An alternative path for the epimerization of  $3_1$  into  $4_1$

in the conventional stereochemistry, because, for example, the descriptor set ( $1R$ ,  $3R$ ) of  $17$  and the descriptor set ( $1S$ ,  $3S$ ) of  $\overline{17}$  are seemingly pairwise to be given a pair of the enantiomers ( $17$  and  $\overline{17}$ ). From the present viewpoint, however, this pairing is not a prerequisite for specifying  $RS$ -stereodescriptors, but only a result derived from the chirality-faithfulness of the priority sequences employed in the processes of specifying respective  $RS$ -stereogenic centers. In fact, the  $1R$ - and  $1S$ -stereodescriptors stem respectively from the  $RS$ -diastereomeric relationships between  $17_{\ell 1}$  and  $16_{\ell 1}$  and between  $\overline{17}_{\ell 1}$  and  $\overline{16}_{\ell 1}$ , which appear in stereoisogram #1 of the correlation diagram shown in Fig. 10b. The  $3R$ - and  $3S$ -stereodescriptors stem respectively from the  $RS$ -diastereomeric relationships between  $17_{\ell 3}$  and  $19_{\ell 3}$  and between  $\overline{17}_{\ell 3}$  and  $\overline{19}_{\ell 3}$ , which appear in stereoisogram #2 of the correlation diagram shown in Fig. 10d.

No  $RS$ -stereodescriptors are assigned to the  $C_2$  atoms of  $17/\overline{17}$  because of the Type II stereoisogram (#2) shown in Fig. 10, where a self- $RS$ -diastereomeric pair  $17_{\ell 2}/18_{\ell 2}$  (or  $\overline{17}_{\ell 2}/\overline{18}_{\ell 2}$ ) is taken into consideration.

### 3 Discussion

#### 3.1 What do $RS$ -stereodescriptors specify?

The procedure based on the correlation diagrams of stereoisograms (Figs. 6, 8, 9, and 10) provides us with an important conclusion as a new viewpoint:

*A pair of  $R$ - and  $S$ -stereodescriptors is given to a pair of  $RS$ -diastereomers generated at each  $RS$ -stereogenic center.*

This fact has been overlooked until now in the conventional stereochemistry, which has been based on another viewpoint that a pair of  $R$ - and  $S$ -stereodescriptors is given to a pair of enantiomers or to a pair of diastereomers.

The digraphs **8** (for **3**) and **9** (for **4**) shown in Fig. 5 demonstrate an implicit violation of the conventional viewpoint. Although **3** is achiral, the promolecules  $3_1$  and  $\overline{3}_1$

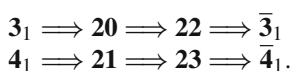
are enantiomeric by adding a solid circle at each  $C_1$  atom, as shown in Fig. 11. On a similar line to the digraph **8** ( $R$ -configuration) derived from  $\mathbf{3}_1$ , the digraph  $\overline{\text{CHClp}\overline{\text{q}}}$  ( $S$ -configuration) is obtained from  $\overline{\mathbf{3}}_1$ , where priority sequence  $\text{Cl} > \overline{\text{p}} > \overline{\text{q}} > \text{H}$  is employed. This sequence is different from the sequence for specifying the  $R$ -configuration or **8**, i.e.,  $\text{Cl} > \text{p} > \text{q} > \text{H}$ . Hence, the conventional viewpoint is found to be based on a presumption that the priority sequence  $\text{Cl} > \overline{\text{p}} > \overline{\text{q}} > \text{H}$  and the priority sequence  $\text{Cl} > \text{p} > \text{q} > \text{H}$  can be used in a pairwise comparison. Logically speaking, the two different priority sequences (though they are correlated to each other) are by no means capable of the pairwise specification of the  $R$ - and  $S$ -configurations.

So long as we rely on the conventional viewpoint, the  $RS$ -stereodescriptors are so impure as to have two different kinds of targets, i.e., a pair of enantiomers and a pair of diastereomers. In contrast, once we rely on the present viewpoint, the  $RS$ -stereodescriptors are so pure as to have a single target, i.e., a pair of  $RS$ -diastereomers. The present approach using correlation diagrams of stereoisograms demonstrates that the conventional viewpoint should be abandoned.

### 3.2 Epimerization processes

The epimerization of  $\mathbf{3}_1$  into  $\mathbf{4}_1$  is regarded as a permutation (1 5) in the stereoisogram shown in the left part of Fig. 6a. This epimerization can be alternatively interpreted to gain more information on the conventional viewpoint. Let us separate the  $\text{Cl}-C_1-\text{H}$  unit from  $\mathbf{3}_1$  so as to generate **20**, as shown in Fig. 11. Then, the residual unit is rotated to generate **21**, which is again combined together to give  $\mathbf{4}_1$ . The residual unit of **20** is identical with the residual unit of **21** so as to demonstrate the  $RS$ -diastereomeric relationship between  $\mathbf{3}_1$  and  $\mathbf{4}_1$ . The epimerization of  $\overline{\mathbf{3}}_1$  into  $\overline{\mathbf{4}}_1$  can be discussed similarly by considering the intermediacy of **22** and **23**.

The conventional viewpoint is explained by the following paths:



The step  $\mathbf{20} \implies \mathbf{22}$  (or  $\mathbf{21} \implies \mathbf{23}$ ) involves a reflection operation of the residual units at issue. Fortunately, the priority sequences in these cases are maintained during the reflection operation. However, this maintenance does not hold true in such cases as containing pseudoasymmetry.

Let us examine the epimerization of  $\mathbf{6}_1$  into  $\mathbf{7}_1$ , as shown in Fig. 12. This can be discussed similarly by considering the intermediacy of **24** and **25**. The epimerization process between the promolecules  $\mathbf{6}_1$  and  $\mathbf{7}_1$  corresponds to an  $RS$ -diastereomeric relationship between them, which are pairwise determined to have  $s$ - and  $r$ -configurations.

Because  $\mathbf{6}_1$  and  $\mathbf{7}_1$  are diastereomeric in terms of the conventional terminology, the result shown in the top row of Fig. 12 is seemingly consistent with the conventional viewpoint that a pair of  $R$ - and  $S$ -stereodescriptors is given to a pair of enantiomers or to a pair of diastereomers. For the purpose of developing a balanced viewpoint, however, Figs. 11 and 12 must be interpreted on a common basis. Hence, if we rely

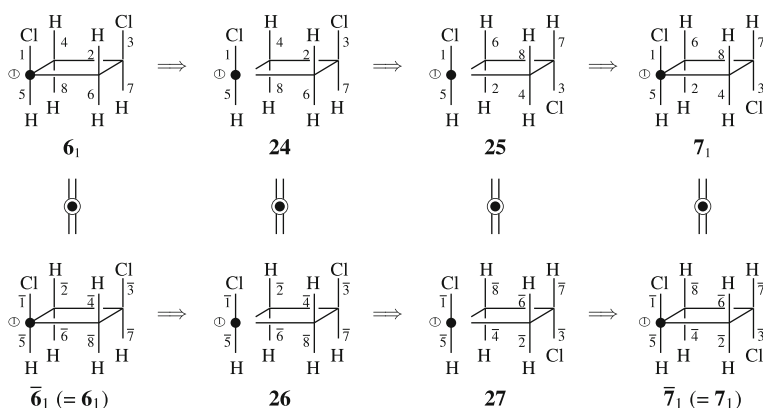
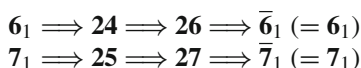


**Fig. 12** An alternative path for the epimerization of  $\mathbf{6}_1$  into  $\mathbf{7}_1$

on the conventional viewpoint and maintain the criterion for interpreting Fig. 11, the following paths must be presumed:



in order to interpret Fig. 12, because the promolecules  $\mathbf{6}_1$  and  $\mathbf{7}_1$  are achiral even if the local symmetries are represented by the promolecules. These paths do not serve as a criterion to give *RS*-stereodescriptors. Obviously, the conventional criterion (aiming at enantiomeric relationships) which is seemingly effective to interpret Fig. 11 is not effective to interpret Fig. 12. Instead, the conventional viewpoint adopts another criterion (aiming at diastereomeric relationships) to interpret Fig. 12. This ad hoc switching contradicts the validity of the conventional viewpoint.

The present approach teaches us that such examinations as illustrated by Figs. 11 and 12 can be conducted systematically by using stereoisograms shown in Figs. 6 and 8.

### 3.3 Over-simplified dichotomy between diastereomers and enantiomers

The conventional stereochemistry relies on the dichotomy between diastereomers and enantiomers, where stereoisomers other than enantiomers are regarded as diastereomers. The correlation diagrams discussed in this article show that such diastereomers are characterized more detailedly. For example, the correlation diagram shown in Fig. 9 shows that diastereomeric relationships concerning  $\mathbf{12}$  can be characterized in terms of *RS*-stereoisomers (enantiomers, *RS*-diastereomers, and holantimers), as collected in Table 1.

In the conventional stereochemistry, all of the six relationship other than the enantiomeric relationship (collected in Table 1) are referred to as diastereomeric relationships. Thus, the conventional dichotomy between enantiomers and diastereomers is concluded to be over-simplified.

**Table 1** Diastereomeric Relationships Concerning **12**

Pair	Relationship	Stereoisogram
Enantiomeric relationship		
<b>12/12</b>	Enantiomeric	Fig. 9a #1
Diastereomeric relationships		
<b>12/13</b>	<i>RS</i> -diastereomeric at C <sub>1</sub>	Fig. 9b #1
<b>12/13</b>	Holantimeric at C <sub>1</sub>	Fig. 9b #1
<b>12/15</b>	<i>RS</i> -diastereomeric C <sub>2</sub>	Fig. 9c #1
<b>12/15</b>	Holantimeric at C <sub>2</sub>	Fig. 9c #1
<b>12/14</b>	Holantimeric at C <sub>3</sub>	Fig. 9d #1
<b>12/14</b>	<i>RS</i> -diastereomeric C <sub>3</sub>	Fig. 9d #1

## 4 Conclusion

Stereoisograms of cyclobutane derivatives are discussed on the basis of their correlation diagrams. The *RS*-stereoisomeric group of a cyclobutane skeleton is constructed by starting from the point group  $D_{4h}$ , where the *RS*-stereoisomeric group is considered to represent a global symmetry. Thereby, stereoisomers derived from the cyclobutane skeleton are treated by a main correlation diagram of stereoisograms under the action of the *RS*-stereoisomeric group. On the other hand, the local symmetry of each *RS*-stereogenic center is discussed on basis of the *RS*-stereoisomeric group of a promolecule generated at the center, where the *RS*-stereoisomeric group for specifying the promolecule is constructed by starting from the point group  $T_d$ . Such promolecules derived from respective stereoisomers are correlated to each other by using stereoisograms, which are further correlated to give a correlation diagram of stereoisograms. *RS*-stereodescriptors are discussed on the basis of such correlation diagrams of stereoisograms.

## References

1. IUPAC Organic Chemistry Division, Pure Appl. Chem. **68**, 2193–2222 (1996)
2. IUPAC Chemical Nomenclature and Structure Representation Division, Provisional Recommendations. Nomenclature of Organic Chemistry, [http://www.iupac.org/reports/provisional/abstract04/favre\\_310305.html](http://www.iupac.org/reports/provisional/abstract04/favre_310305.html) (2004)
3. R.S. Cahn, C.K. Ingold, V. Prelog, Angew. Chem. Int. Ed. Eng. **5**, 385–415 (1966)
4. V. Prelog, G. Helmchen, Angew. Chem. Int. Ed. Eng. **21**, 567–583 (1982)
5. K. Mislow, J. Siegel, J. Am. Chem. Soc. **106**, 3319–3328 (1984)
6. S. Fujita, J. Org. Chem. **69**, 3158–3165 (2004)
7. S. Fujita, J. Math. Chem. **35**, 265–287 (2004)
8. S. Fujita, MATCH Commun. Math. Comput. Chem. **61**, 11–38 (2009)
9. S. Fujita, *Symmetry and Combinatorial Enumeration in Chemistry*, (Springer-Verlag, Berlin-Heidelberg, 1991)
10. S. Fujita, Helv. Chim. Acta **85**, 2440–2457 (2002)
11. S. Fujita, J. Math. Chem. **33**, 113–143 (2003)
12. S. Fujita, MATCH Commun. Math. Comput. Chem. **53**, 147–159 (2005)
13. S. Fujita, MATCH Commun. Math. Comput. Chem. **54**, 39–52 (2005)
14. S. Fujita, Tetrahedron **62**, 691–705 (2006)